Journal of Advances in Computer Research
Quarterly pISSN: 2345-606x eISSN: 2345-6078
Sari Branch, Islamic Azad University, Sari, I.R.Iran
(Vol. 6, No. 3, August 2015), Pages: 65-85
www.jacr.iausari.ac.ir

Random Texture Defect Detection by Modeling the Extracted Features from the Optimal Gabor Filter

S.Abdollah Mirmahdavi[1],Abdollah Amirkhani✉[2],Alireza Ahmadyfard[1],M. R. Mosavi[2]

1) Dept. of Electrical & Robotic Engineering, Shahrood University of Technology, Shahrood, Iran
2) Dept. of Electrical Engineering, Iran University of Science and Technology, Tehran, Iran

mmirmahdavi@shahroodut.ac.ir; amirkhani@ieee.org; ahmadyfard@shahroodut.ac.ir, m_mosavi@iust.ac.ir

Received: 2014/07/25; Accepted: 2014/10/08

Abstract

In this paper, a new method is presented for the detection of defects in random textures. In the training stage, the feature vectors of the normal textures' images are extracted by using the optimal response of Gabor wavelet filters, and their probability density is estimated by means of the Gaussian Mixture Model (GMM). In the testing stage, similar to the previous stage,at first, the feature vectors corresponding to local neighborhoods of each pixel of the image under inspection are extracted. Then, by computing the likelihood of the test image's feature vectors' belonging to the parameters of the GMM, they are compared with a threshold value. Finally, the defective regions are localized in a defect map. The proposed algorithm was evaluated on a set of grayscale ceramic tile images with random textures. The simulations indicate that in comparison with the previous methods, the proposed algorithm enjoys an acceptable computational volume and accuracy in the detection of texture defects.

Keywords:*Defect detection, Random texture, Gabor wavelet filters, Gaussian mixture model*

1. Introduction

The primary objective of performing automatic visual inspection of various surfaces is to find regions of these surfaces whose apparent or physical characteristics based on certain criteria such as color or pattern regularity deviate from the normal characteristics of the corresponding regions in the training and flawless samples. Nowadays, methods based on machine vision are commonly used for detecting and locating such flaws and defects in various applications, such as in the inspection and quality control of the surfaces of ceramic tiles [1], textiles [2] and silicon wafers [3]. Generally, these detection processes are classified within the domain of texture analysis. From the perspective of apparent looks, the textures are normally classified into regular textures and random textures [4]. Unfortunately, many of the defect detection techniques for regular textures cannot be easily applied to random textures. Because in many of these methods, the inherent regularity or repeating characteristic of the given textures are used for the detection of defects; while in random textures, usually there are no obviously regular or repeating patterns. So it is very important to devise and present novel detection methods in this regard. Figure 1 shows the images of a defective regular texture and a defective random texture. Since the regular texture has a periodic structure

in Figure 1.a, it is much easier to find the target defect in it compared to the random texture. In fact, the defective regions in random textures may be counted as the main patterns of the flawless texture. Therefore in such cases, it is essential to differentiate the defect from the main texture pattern. It is obvious that this dilemma makes the process of defect detection in random textures more complicated.

Contrary to regular textures, few methods have been presented so far for the detection of defects in random textures. The most recent and significant approaches that exist on this subject will be covered in the following section. A method of detecting defects in random textures based on the T^2 statistics has been presented in [5]. In the training stage of this method, the PCA analysis is used to extract a reference Eigenspace from a particular matrix known as the data matrix. The elements of this matrix are obtained from a specific arrangement of the grayscale values of the existing pixels in the neighborhoods of a set of flawless images in three color channels (R, G, B). This reference Eigenspace actually determines the normal behavior of the pixels within the neighborhood of trained flawless textures. Also in the testing stage, the mentioned data matrix is constructed from the test image, in a manner similar to the training stage, and then it is mapped into the Eigenspace obtained from the training stage. Then for each pixel, distance T^2 is calculated and compared to a threshold value. Pixels whose T^2 distances are larger than this permitted limit are marked as defective pixels. Unfortunately, a very large volume of computations has been reported for this approach.

The method proposed in [6] is based on the modeling of random textures for the detection of defective regions. Through this approach, the textural primitive of a reference image or a set of reference images are represented as TEXEMs. In this method, first, the local neighborhoods of the reference images are modeled by means of the GMM, and the parameters of this model are determined by the EM algorithm. Ultimately, the mean and variance of this Gaussian Mixture Model (GMM) are considered as TEXEMs. This local analysis of image is applied to a set of grayscale ceramic tile images by means of TEXEMs, in which the grayscale information is sufficient to correctly identify the defects. This scheme is then extended to include the color images as well. This strategy leads to various formulations and deduction procedures, and different computational complexities. Finally, the proposed method is implemented in the form of a novelty detection strategy in order to be flexible in detecting various defects, which are mostly unpredictable.

The method proposed in [7] includes two stages of training and testing. In the training stage, the textural pattern of a number of normal textures in the form of local neighborhoods is taught to a number of hidden Markov models. The structure as well as the quantity of these models is determined automatically and optimally. Then in the testing stage, these models are used for the detection of defects in local neighborhoods. Also, for the detection of different size defects, the proposed method has been implemented in a multi-scale framework.

(a) (b)

Figure 1.An example of a defective regular texture (a) and a defective random texture (b). The defects of each image have been marked by elliptical lines.

In [8], the authors have used the Gabor filters to extract the feature vectors and Self-Organizing Maps (SOMs) in order to detect the defects on the surface of tiles containing random textures. However, despite the simplicity and small computational volume of this method, the authors of this article have not stated any degree of accuracy for this method compared to other approaches.

In the current paper, a new method for the modeling of random textures in the spatial-frequency domain is presented for the detection of defects on the surfaces of these types of textures. One of the applications of texture defect detection is in the processes of surface inspection in various industries. These processes are generally recognized as online and real time implementations, and therefore, the processing time plays a very important role in the practicality of an inspection method. Hence, the speed of execution of the proposed method must be high enough so that it can be implemented as a real time system. It should also be noted that in many real applications, the probable defects on surfaces are unpredictable and it is practically impossible to have all the possible defects in order to train a defect detection system. So the proposed system should be automatic as much as possible, and it should not need to be trained on a defective class. Therefore, in a training process, the considered system can be trained by samples of a flawless class or group; and in the testing stage, the system can automatically detect and localize the possible defects. It should be mentioned that in many applications, it is not merely sufficient to determine whether a texture is flawless or defective; and it would be necessary to know the position as well as the size of the defects. These defects could come in very small to very large sizes, and therefore the proposed method must be capable of detecting and localizing different types of defects at various sizes. In this article, in the training stage, the feature vectors extracted from the optimal response of the Gabor wavelet filter of a number of flawless samples are trained by the GMM; and in the testing stage, by using the parameters of the trained model and an optimum threshold value, the defects on the surface of image under inspection are detected and localized. Also in this article, a new method of choosing the optimum of the Gabor wavelet filter has been presented for detecting the defects of random textures.

In continuation, the concepts of Gabor wavelet filters and Gaussian mixture model will be reviewed in Section 2, and then the proposed method will be introduced in Section 3. Finally, the experimental results and the conclusion will be presented in Sections 4 and 5, respectively.

2. Background review

2.1. Gabor wavelet filters

Gabor filters are amongst the most important filters in the field of defect detection. The two-dimensional Gabor filters are frequency- and direction-sensitive band-pass filters which have been optimally defined in the frequency and space domains, and which are appropriate for the extraction of direction-dependent frequency content [9]. The two-dimensional Gabor filter in the space domain consists of a Gaussian function modulated with a mixed sine function, which is defined as equation (1):

$$g(x,y) = \frac{1}{2\pi\sigma_x \sigma_y}.\exp\left[-\frac{1}{2}\left(\frac{x^2}{\sigma_x^2}+\frac{y^2}{\sigma_y^2}\right)\right]\cdot\exp\left[j2\pi(Wx)\right] \quad (1)$$

In the above equation, W is the frequency of the sine function in the Cartesian coordinates, and σ_x and σ_y are the standard deviations of the Gaussian envelope function along the x and y axes, respectively. The family of Gabor wavelets or a bank of Gabor filters is obtained by scaling and orienting the mother Gabor wavelet $g(x, y)$ according to the following equations [10]:

$$g_{mn}(x,y) = \alpha^{-m}\ g(\tilde{x},\tilde{y}), \quad m = 0,1,2,...M-1 \quad , \quad n = 0,1,2,...N-1 \quad (2)$$

$$\tilde{x} = \alpha^{-m}(x\cos\theta + y\sin\theta) \quad (3)$$

$$\tilde{y} = \alpha^{-m}(-x\sin\theta + y\cos\theta) \quad (4)$$

$$\theta = \frac{n\pi}{N} \quad (5)$$

In the above equations, g_{mn} is the filter scaled and oriented from the mother filter $g(x, y)$. Subscripts m and n indicate the scale and orientation, respectively. In addition, M and N express the total number of scales and total number of orientations, respectively. The numbers of directions and scales vary in different applications, and it is very important to choose these numbers precisely in order to achieve the desired objective. Until now, no structured and standard way of choosing the number of directions and scales has been presented and almost all these selections are done empirically through trial and error. The designing of filter banks requires an extensive set of predetermined parameters to effectively cover the pattern frequency and texture design. The goal of using a filter bank instead of a filter at a specific direction and scale is to be able to analyze the images at different directions and scales. Generally, the Gabor wavelet function strongly depends on the four parameters of w, α, σ_y and σ_x; and small changes in these parameters can drastically affect the operation of the filter. Therefore, the

accurate calculation of these parameters can be very useful in minimizing the error of defect detection.

The non-orthogonality of the Gabor wavelets leads to redundant information. Therefore, in order for the filter output to have the most useful and the least excessive information, the following formulas are used for the design [11]:

$$\delta_{x,mn} = \frac{(\alpha+1)\sqrt{2\ln 2}}{2\pi\alpha^m(\alpha-1)U_l} \tag{6}$$

$$\delta_{y,mn} = \frac{1}{2\pi\tan\left(\frac{2\pi}{N}\right)\sqrt{\frac{U_h^2}{2\ln 2}-\left(\frac{1}{2\pi\delta_{x,mn}}\right)^2}} \tag{7}$$

$$W_{mn} = \alpha^m U_l \tag{8}$$

$$\alpha = \left(\frac{U_h}{U_l}\right)^{\frac{1}{M-1}} \tag{9}$$

where $U_l$and U_h are the lowest and highest central frequencies of the considered filter bank, and W_{mn} (with scale m and direction n) is the central frequency of each filter of the filter bank. With regard to the above structure and by tuning the U_l, U_h, M and N parameters, the desired filter bank can be designed.

The existing pixels in an image can be classified into flawless and defective pixels considering the local response of the filter to those pixels. To determine the frequency response for every pixel of an image, the image can be convoluted by the Gabor wavelet filters. By convoluting each image with the real and imaginary sections of the Gabor wavelet filter, the pixels of the image can be described by extracting some features from the image obtained by the process of convolution. Equation (10) is obtained by applying the $g_{mn}(x, y)$ filter to image $I(x,y)$.

$$h^T{}_{mn}(x,y) = \sum_s \sum_t I(x-s, y-t) g^*{}_{mn}(s,t) \tag{10}$$

According to this process, each of the images obtained from the application of filter bank consists of a set of responses, which are represented in the form of $H^I = \{h_{mn}{}^I, m = 1, 2, \ldots, M; n = 1, 2, \ldots, N\}$ and which contain the information of the image at a specific scale and direction.

2.2. Optimal Gabor filter

The objective of using a filter bank instead of a single filter at a specific direction and scale is to be able to analyze an image at different directions and scales. A filter at a certain direction and scale can extract only a portion of an input image's characteristics; while a filter bank can display the image's characteristics at various directions and scales. Then by using the existing approaches, the best response among the filters can be obtained and the optimal filter can be chosen.

There are different methods for determining the best response from among the filters used in a filter bank [12]. A new and effective method has been presented in this article for selecting the optimal response of the Gabor filter bank in order to detect the defects on the surfaces of random textures.

As the following section indicates, the feature vectors that are extracted in the training and testing stages comprise the pixel values of the Gabor wavelet filter's optimal response. Since the values chosen for the flawless regions should be different from those chosen for the defective regions, so a response should be sought in the Gabor wavelet filter bank which can properly differentiate between the flawless and defective regions. In the algorithm for the extraction of optimal response, first, the Gabor wavelet responses of every image are averaged according to equation (11).

$$\bar{h}^I(x,y) = \frac{1}{M \times N} \sum h^I_{m,n} \tag{11}$$

The output of the Gabor wavelet filter of a tile's image and of the image of its average responses has been shown in Figure 2.

To choose the best response from the set of H^I observations, the criterion of similarity or closeness of the Gabor wavelet responses to the average image calculated in equation (11) is used. In order to determine the distance between these two, the criterion function of Chi-2 (χ^2) is used [13]:

$$\chi^2(h_{m,n}, \bar{h}^I) = \sum_{i=1}^{S} \frac{(h_{m,n} - \bar{h}^I)^2}{|h_{m,n}| + |\bar{h}^I|} \tag{12}$$

where S signifies the number of pixels of the Gabor wavelet responses. For a set of responses of the Gabor wavelet filter bank, the filter is selected as the optimal filter whose corresponding response has the farthest distance from the average value. Therefore, in view of what is said, the chosen optimal filter is F_{kl}, which has the best response in the equation to the input image.

$$F^I_{kl} = \max_{m,n} \left\{ \chi^2(h_{m,n}, \bar{h}^I) \right\} \tag{13}$$

Therefore, the optimal response of the chosen filter (indicated by $h_{kl}{}^I(x, y)$) can be obtained from the set of H^I observations. The acquired optimal response is used for the extraction of feature vectors. The results of the proposed method for the extraction of the Gabor wavelet filter's optimal response indicate that this method is well capable of detecting the defects of random textures.

2.3. Gaussian mixture model

The GMM is an unsupervised clustering method based on the assumption of Gaussian distribution for the input data. The Gaussian mixture model has an adequate capability in modeling the kinds of phenomena that have a natural distribution and irregular data. This characteristic has enabled the GMM method to be employed todayas the main tool in speaker identification systems and also as a reference system inmanyhybrid models. It is also used as a reference model, for comparison purposes, in manybiometric tests [14].

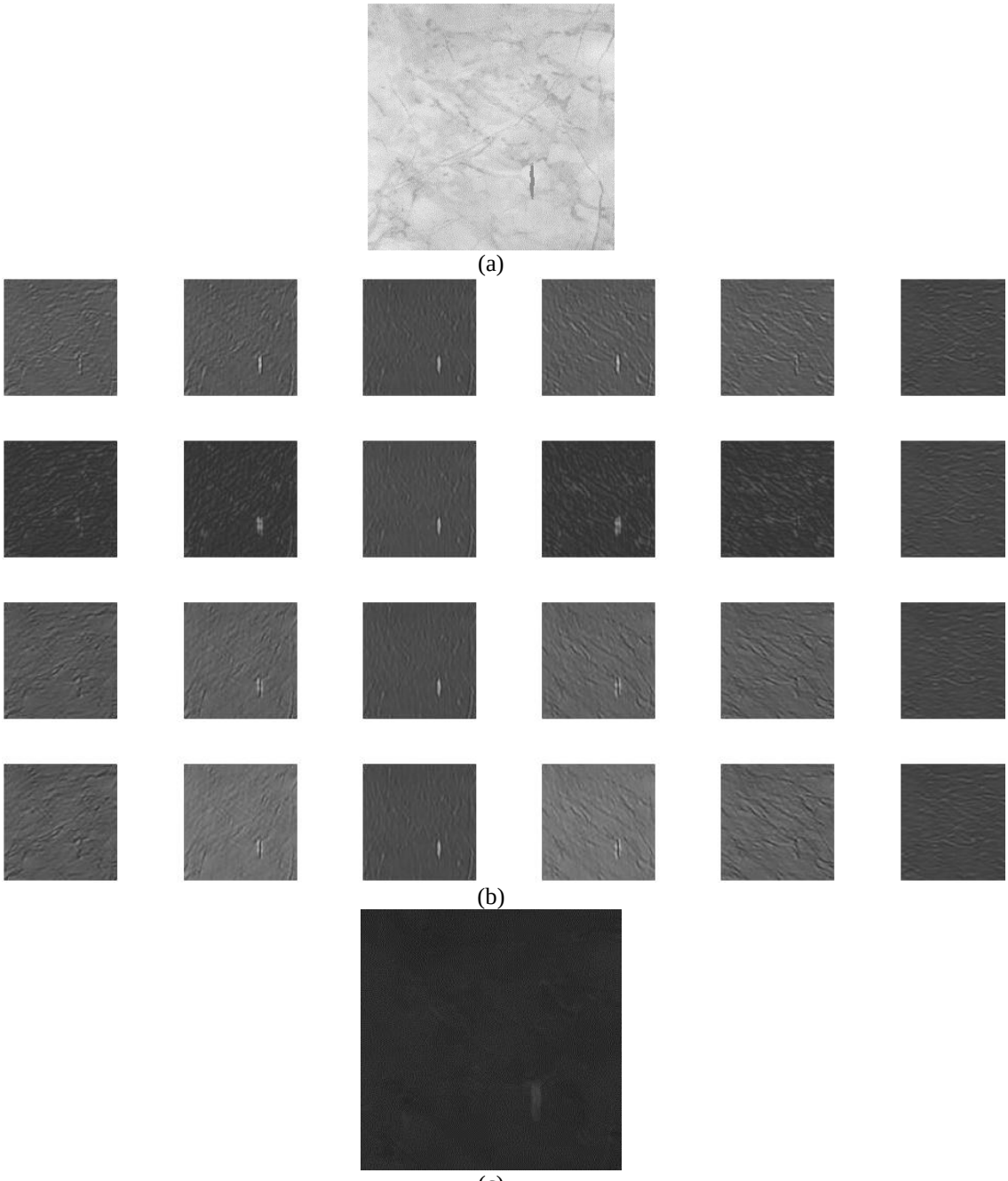

Figure 2. (a) Image of a defective tile's random texture, (b) Responses of the Gabor wavelet filters of Fig. 2(a) at 4 scales and in 6 directions, (c) Average image of the Gabor wavelet filters response

The density function of the Gaussian mixture model is obtained from the weighted set of K Gaussian distributions, according to equation (14):

$$p(\vec{x} \mid \psi) = \sum_{i=1}^{K} g\left(\vec{x} \mid \mu_i, \Sigma_i\right) \alpha_i . \tag{14}$$

With regard to equation (14), x is the d-dimensional feature vector, α_i is the weight of the i^{th} mixture, and g(x/ μ_i, Σ_i) denotes a fraction of the Gaussian mixture density with

average μ_i and covariance matrix Σ_i. The weight of each fraction is determined based on the probability of occurrence of that fraction with respect to the training data. Each density fraction is a d-dimensional Gaussian function, which is defined as equation (15):

$$g(\vec{x} \mid \mu_i, \sum_i) = \frac{1}{(2\pi)^{D/2} \left|\sum_i\right|^{1/2}} \times \exp\left\{-\frac{1}{2}(\vec{x} - \mu_i)^T \sum_i{}^{-1} (\vec{x} - \mu_i)\right\} \quad (15)$$

Therefore, the GMM model can be defined by the parameters of mean vector, covariance matrix and by the weight of each partial mixture density; and the goal is to find these parameters ($\Psi = \{\alpha_i, \mu_i, \Sigma_i\}_{i=1}^{k}$). There are numerous methods for the estimation of the Gaussian model's parameters. One of the most common of these approaches is the use of Expectation Maximization Algorithm.

3. The proposed method

It seems that the global textural pattern that exists in random textures follows an undefined random process. This assumption has been considered in many different applications of the Gaussian mixture model, such as speech processing. Since the Gaussian mixture model is a very powerful tool for the modeling and analysis of arbitrary and random processes, the GMM method has been used in this article for the modeling of random textures. The important point that should be mentioned is that the obtained model parameters may have no physical and external meaning and may only denote the clustering property of the feature vectors or the observations. This notion is also true in the methods proposed in this article. In fact, it can be presumed that in the proposed method, the parameters of the GMM will be used as textural feature descriptors.

It has been demonstrated in [15] that many of the real signals can be investigated and analyzed by studying their local neighborhoods. The obtained findings indicate that textures with global structures can be differentiated from one another by analyzing the distribution of their local features. In this research, this notion will be applied as the basic principle. The use of Gabor wavelet filters gives us the opportunity to also consider the frequency contents of the texture as well as the methods for the extraction of features in the spatial domain (such as the GLCM) [16], and to present a more accurate description of the surface features of these random textures.

The block diagram of the proposed method has been shown in Figure 3, which consists of two stages of training and testing. Each of these stages will be explained separately in the next sections.

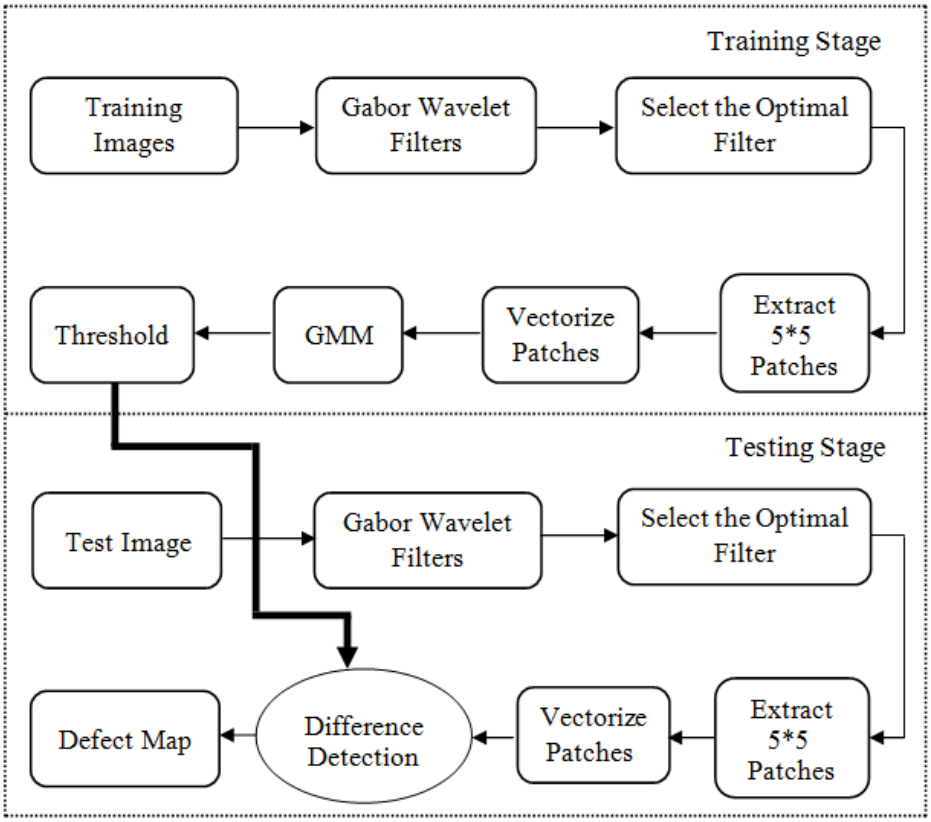

Figure 3. Block diagram of the proposed method.

3.1. The training stage

In this research, the idea of novelty detection [17] is used, which constitutes a different method among the common clustering approaches for the detection of defects in surface textures. In this method, in the training stage, flawless samples are used instead of defective ones. Due to the haphazard and unpredictable nature of defects in many applications, it is rather difficult to get enough defective samples and to produce a set of defective training data that can cover all the characteristic space of this class. However, the novelty detection approach only uses the data from flawless samples in the training stage in order to model these data. From a geometrical perspective, in the N-dimensional space of features, the flawless samples produce concentrated clusters; while the defective samples can be scattered throughout the whole space and be away from the centers of flawless texture clusters [18]. So in this research, the images of flawless textures, which all are of the same family, are used as inputs and the features extracted from each of these images are employed for modeling and for finding the threshold limit.

3.1.1. Feature extraction

At this stage, the texture image is described by the windows extracted from the optimal response of the training image's Gabor wavelet. To this end, first, the image of the Gabor wavelet's optimal response is divided into smaller 5x5 windows that do not

overlap. The interesting point is that the image of the Gabor wavelet's optimal response does not exclusively contain positive values, and if we keep plotting the surface of the image obtained from the convolution operation, we shall see that this surface again includes both positive and negative values. This occurs because of performing the convolution between the image normalized by negative values and the filters that contain positive as well as negative values. Figure 4 shows an example of the mentioned trend.

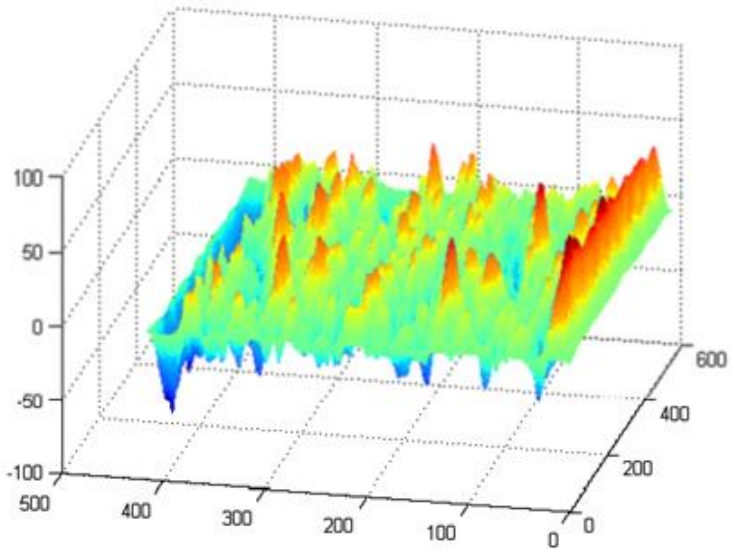

Figure 4. Procedure related to the response of one of the Gabor wavelet filters, before measuring the size of the pixels.

The trend plotted above shows the changes of the texture, and these changes become more severe in some regions. The interesting point in this regard is that if we exclude the existing changes at the beginning and end of the trend, which are due to the effect of image edges, the remaining drastic changes will correspond to the plausible defective regions, which in view of the reason given above, a portion of them falls in the positive region and another portion in the negative region. Conversely, the output image, due to being convoluted by the Gabor wavelet filter, will have a mixed form again; because the existence of an exponential term in the filter's formulation ensures the mixed form of the final image. Therefore, if instead of using pixel values, pixel sizes are used, not only the imaginary part will be eliminated, but also the negative regions, which create the basins, will turn into domes. For 5x5 windows, a 25-element feature vector describes the windows extracted from the optimal response of the flawless texture's Gabor wavelet.

$$\vec{x}_t = [Q_1, Q_2, ..., Q_{25}] \tag{16}$$

Figure 5 shows the flowchart used for the extraction of feature vectors. In continuation, the probability density of the feature vectors corresponding to all the flawless texture windows extracted from $h_{kl}^{I}(x, y)$ is estimated by means of the GMM.

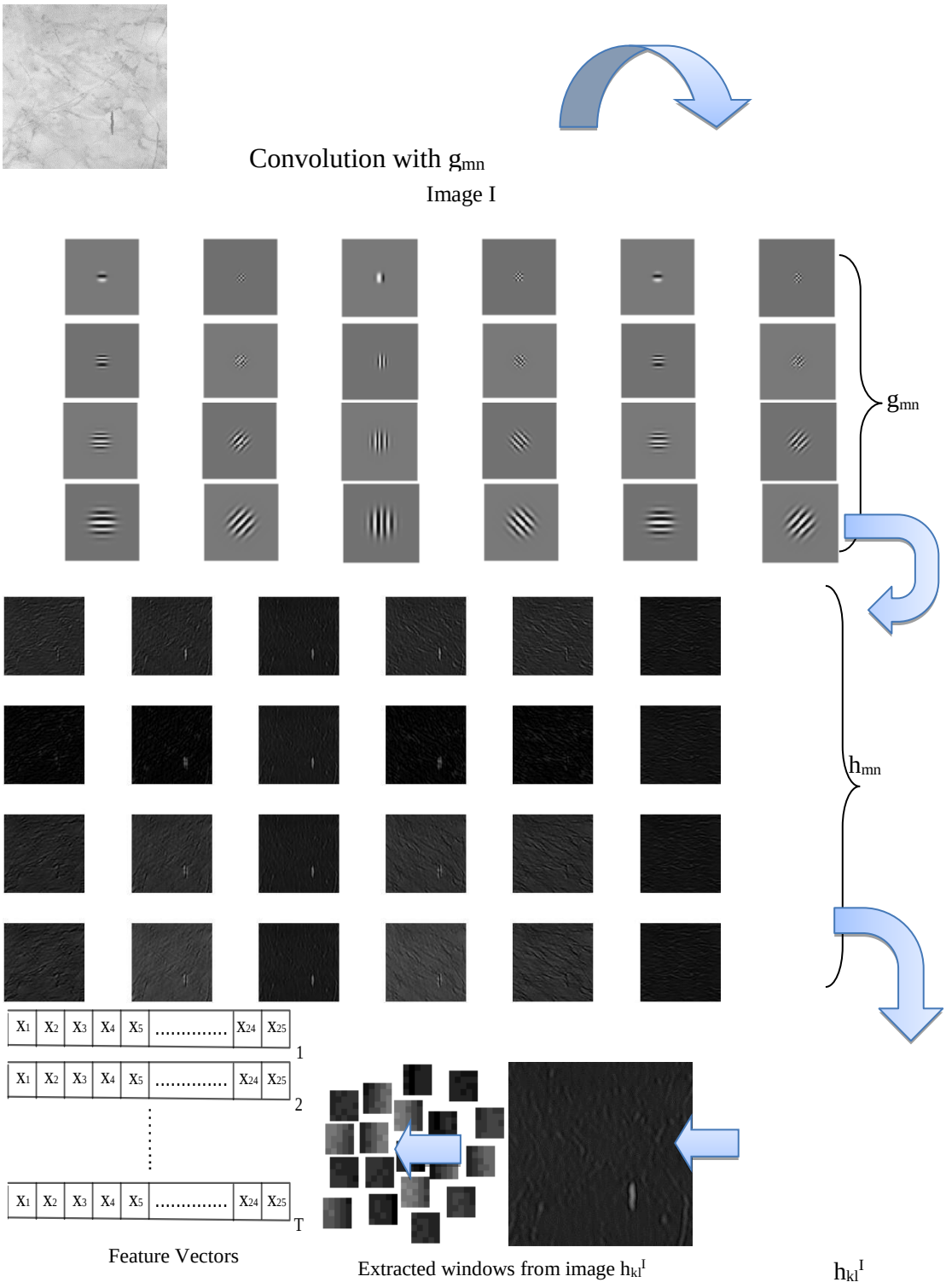

Figure 5. Flowchart for the manner of extraction of feature vectors.

3.1.2. Modeling the feature vectors by GMM

At this point, the probability density of the feature vectors belonging to a flawless texture image, which had been extracted according to the procedures described in the previous section, is estimated by the Gaussian mixture model, and the parameters of the GMM are resulted from this probability density. In this model, it is assumed that every feature vector x_t in the N-dimensional space is produced by a probability density function. Obviously, the obtained model can model the behavior of the defect-free texture's image characteristics. It should be mentioned that due to the similarity of the feature vectors of a family of random textures, and the fact that these vectors cannot be good representatives for the modeling of other textures belonging to the same family, and in order to reduce the volume of computations, only the feature vectors of a flawless image have been used for modeling.

In addition, it should be stated that in a system based on the Gaussian mixture model, the probability distribution of the flawlesstexture's feature vectors $X = \{x_t, 1 \le t \le T\}$ is expressed as a linear combination of K Gaussian mixtures, according to equation (17):

$$p(\vec{x}_t \mid \psi) = \sum_{i=1}^{K} g\left(\vec{x}_t \mid \mu_i, \Sigma_i\right) \alpha_i \tag{17}$$

Ψ denotes the parameters of the GMM. In this case, it has been assumed that each feature vector is a d-dimensional probability density function (based on what was mentioned in the previous section, D = 25) with the average vector of μ_i and the covariance matrix Σ_i, according to equation (18).

$$g(\vec{x}_t \mid \mu_i, \sum_i) = \frac{1}{(2\pi)^{D/2} \left|\sum_i\right|^{1/2}} \times \exp\left\{-\frac{1}{2}(\vec{x}_t - \mu_i)^T \sum_i{}^{-1} (\vec{x}_t - \mu_i)\right\} \tag{18}$$

By having a series of observations $X = \{x_t, 1 \le t \le T\}$, the likelihood of X for the parameters of the GMM is expressed by equation (19):

$$p(X \mid \psi) = \prod_{t=1}^{T} p(\vec{x}_t \mid \psi) \tag{19}$$

As was explained in the previous sections, by applying the EM algorithm, the maximum likelihood value can be obtained and the model parameters can be estimated. In this regard, the algorithm for the modeling of a flawless texture's feature vectors is expressed as follows:

1) Determining the number of Gaussian mixtures (K), and also performing an initial estimation of the mean parameters (μ^0_i), covariance matrix (Σ^0_i) and the weight of mixtures (α^0_i), which are obtained by the k-means method.
2) Applying step E of the EM algorithm and computing the value of posteriori probability for the ith mixture component, according to equation (20).

$$\Pr(i \mid \vec{x}_t, \psi^n) = \frac{g(\vec{x}_t \mid \mu_i^n, \sum_i^n)\alpha_i}{\sum_{i=1}^{K} g(\vec{x}_t \mid \mu_i^n, \sum_i^n)\alpha_i} \tag{20}$$

3) Applying step M of the EM algorithm and updating the values of mean parameters, covariance matrix and the weights of mixture densities, according to following equations:

$$\alpha_i^{n+1} = \frac{1}{T}\sum_{t=1}^{T} \Pr(i \mid \vec{x}_t, \psi^n) \tag{21}$$

$$\mu_i^{n+1} = \frac{\sum_{t=1}^{T} \Pr(i \mid \vec{x}_t, \psi^n)\vec{x}_t}{\sum_{t=1}^{T} \Pr(i \mid \vec{x}_t, \psi^n)} \tag{22}$$

$$\sum\nolimits_i^{n+1} = \frac{\sum_{t=1}^{T} (\vec{x}_t - \mu_i^{n+1})(\vec{x}_t - \mu_i^{n+1})^T \Pr(i \mid \vec{x}_t, \psi^n)}{\sum_{t=1}^{T} \Pr(i \mid \vec{x}_t, \psi^n)} \tag{23}$$

4) Computing the log-likelihood function of log $p(X / \Psi)$ by means of the updated parameters, via equation (24).

$$\log\, p(X \mid \psi) = \sum_{t=1}^{T} \log\left(\sum_{i=1}^{K} g\left(\vec{X} \mid \mu_i, \Sigma_i\right) \alpha_i \right) \tag{24}$$

6) Repeating steps 3 through 5 until the likelihood logarithmic function converges.

7) Saving the parameters of the converged model (α, μ, Σ).

So according to the abovementioned algorithm, in the training stage, the feature vectors extracted from a flawless training texture are trained in the form of local neighborhoods by the Gaussian mixture model, and the model parameters $\Psi = \{\alpha_i, \mu_i, \Sigma_i\}^k_{i=1}$ are computed and saved.

3.2. Computing the threshold

Now by using the feature vectors from 3 flawless texture images extracted in the first stage and the parameters of the trained model, the threshold boundary is automatically calculated at the testing stage, in order to determine the defectiveness or flawlessness of the pixels of the image under inspection. First, the weighted Euclidian distance of each feature vector extracted from flawless texture images is computed from the parameters of the GMM, according to equation (25).

$$dist(\vec{x}_t, \psi) = \sum_{k=1}^{K} \left(\alpha_k \sqrt{\sum_{n=1}^{N} \frac{(x_n - \mu_{kn})^2}{\delta_{kn}^2}} \right). \tag{25}$$

where K is the total number of Gaussian mixtures, N is the number of existing elements in the feature vectors (N = 25), α_k is the weight of Gaussian mixture, and μ_k and δ_k^2 are the mean vector and the variance of the k^{th} portion of the Gaussian mixture, respectively. Since a smaller distance indicates a higher dependency of the relevant feature vector on the model parameters obtained from the feature vectors of flawless

textures, and since defective samples can be away from the centers of flawless texture clusters, the highest value from the set of these distances can be considered as a border between defective and flawless regions. For comparison purposes, the Euclidian distances of the flawless and the defective regions' feature vectors from the obtained model parameters have been exhibited in Figure 6.

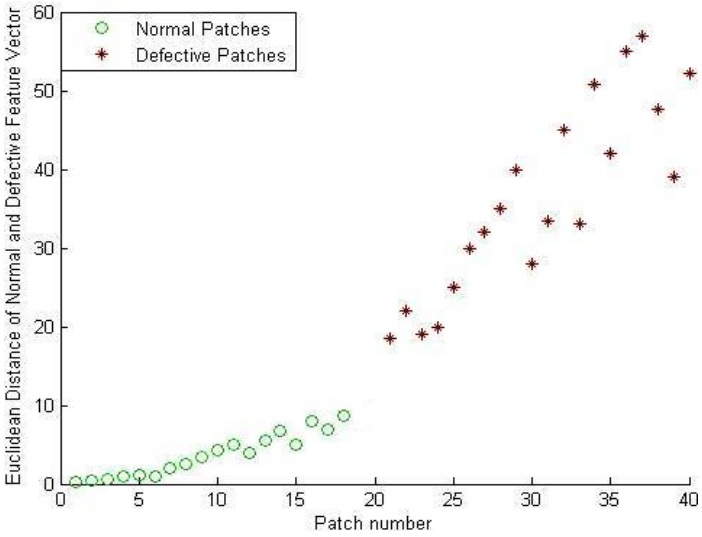

Figure 6. The Euclidean distance of a number of flawless and defective windows from the parameters of the extracted model.

In view of Figure 6, it can be observed that the feature vectors associated with defective regions are more distant from the model parameters. To find the value of the threshold boundary automatically, and without supervision, the K-means clustering algorithm is used. In this method, it is assumed that each obtained values of distance belong to clusters with the mean μ and standard deviation δ. These distance values are divided into L clusters (empirically, L = 5) and then the parameters of a cluster that has the highest mean is considered. These parameters include the standard deviation of the considered cluster (δ_l) and the mean value of the cluster (μ_l). Thus, the boundary between the defective and flawless regions, i.e., the threshold boundary, can be calculated by equation (26).

$$\Upsilon = \mu_l + \lambda\delta_l \tag{26}$$

where λ is a constant coefficient which is determined empirically, and in performing the experiments, its value has been considered as λ =1.25.

3.3. The testing stage

At this stage, like at the training stage, at first, the filter bank of Gabor wavelet is applied to the image under inspection, and the Gabor wavelet's optimal response is determined. For every pixel in the input image, a window is delineated from the center of the pixel with the size of the Gabor wavelet's optimal response in such a way that the feature vector that describes that pixel is formed. After extracting the feature vectors of the image under inspection, the distance of each of these vectors from the model parameters is computed by equation (25). If the distance of each feature vector from the

model parameters is larger than the threshold boundary value (Υ), the pixel related to its corresponding feature vector is considered as the defective region. In this case, a final defect map in binary form can be generated through equation (27) and the defective pixels of the image under inspection can be localized and marked.

$$D(x,y)=\begin{cases}0 & dist(x,y)\geq \Upsilon \\ 1 & dist(x,y)<\Upsilon\end{cases} \quad (27)$$

According to equation (27), *dist*(*x*, *y*) is the distance of the feature vector belonging to the pixel of the image under inspection in the (*x*, *y*) coordinates.

4. Experimental results

With the aim of quantitative and qualitative analysis, the proposed method was applied to a set of grayscale images of ceramic tiles with random textured surfaces. This set consisted of 10 different families of tiles with different designs. There were 1100 images in total with the size of 256x256 pixels each; 150 of these images are flawless and defect-free and the remaining 950 have various defects in their surface textures. These defects come in different sizes and types and they can include physical as well as textural defects. These defective images are used to construct binary images known as the ground-truth maps. In this operation, with the help of an observer or human operator, the defective locations are labeled and marked by hand in a separate image called the ground-truth map. Therefore, a ground-truth map is in fact a binary image corresponding to an image of the defective texture.

One of the parameter that should be determined in the proposed method is the selection of the number of Gaussian mixtures used for modeling. So by performing various experiments, seven Gaussian mixtures (K = 7) were chosen for the modeling of flawless textures. In most of the published articles, depending on the type of application and also the type of texture, the number of Gaussian mixtures is selected empirically and through trial and error, and this quantity of mixtures should be able to cover the whole space of feature vectors. Underestimating the number of Gaussian mixtures leads to inappropriate modeling by the GMM, and overestimating it leads to the increase in the volume of computations and the processing time. Figure 7 shows the effect of the number of Gaussian mixtures on the detection of defects in a random textured tile, for different values of k.

In this research, windows with dimensions of N = 5 x 5 have been employed for the extraction of feature vectors at the training and testing stages. The dimensions of windows should be selected in a way that windows could contain the details of the Gabor filter's optimal response and so that there would be a compromise between the accuracy and the speed of computations [19]. The determination of the exact locations of defects mostly requires that the filters be used in a particular space.The determination of the parameters of Gabor filters that form the filter bank involves the selection of the frequencies and orientations of each of these filters so that the frequency domain can be covered as much as possible by the said filter bank and the texture information can be adequately extracted. The central frequencies of the designed filters should be close enough to the textures' frequency characteristic; otherwise, the texture-to-filter response level will drop sharply.

(a) (b) (c)

Figure 7. The effect of the number of Gaussian mixtures (k) on a tile's defective random texture: (a) The defective texture, (b) Applying the proposed method with k = 7 on the image of texture in (a), (c) Applying the proposed method with k = 4 on the image of texture in (a).

The closer a texture's frequency characteristic is to that of a filter, the higher the response level of the mentioned texture will be to that filter. Therefore in this research, considering the abovementioned and various performed experiments, U_L = 0.1 and U_h = 0.4 were considered as suitable choices for determining the central frequencies. Also the number of filter bank elements in this research is 24 filters, which have been designed in 4 scales and 6 orientations. It should be noted that choosing a large number of filter bank elements produces extra information and causes the computation volume to increase. Conversely, the choice of a small number of filters for the filter bank leads to the loss of textural details. Figure 8 shows examples of the quality of defect detection by the method proposed in this research.

As these figures explicate, the textural patterns of the flawless textures differ from those of defective textures, but in appearance, they seem to have the same textural patterns. These examples demonstrate the ability of the proposed approach in detecting the defects which may range from small to large sizes. To evaluate the accuracy and performance of the proposed method, it is applied on a set of images in the database. The acquired defect maps are then compared with the ground-truth maps that correspond to the image of each test texture, and the results of comparison are quantified with the aid of three criteria of sensitivity, specificity and accuracy. Sensitivity indicates the degree of correct detection of defective pixels; specificity shows the degree of correct detection of flawless pixels; and accuracy expresses the extent of correct detection of all the existing pixels in the considered image.

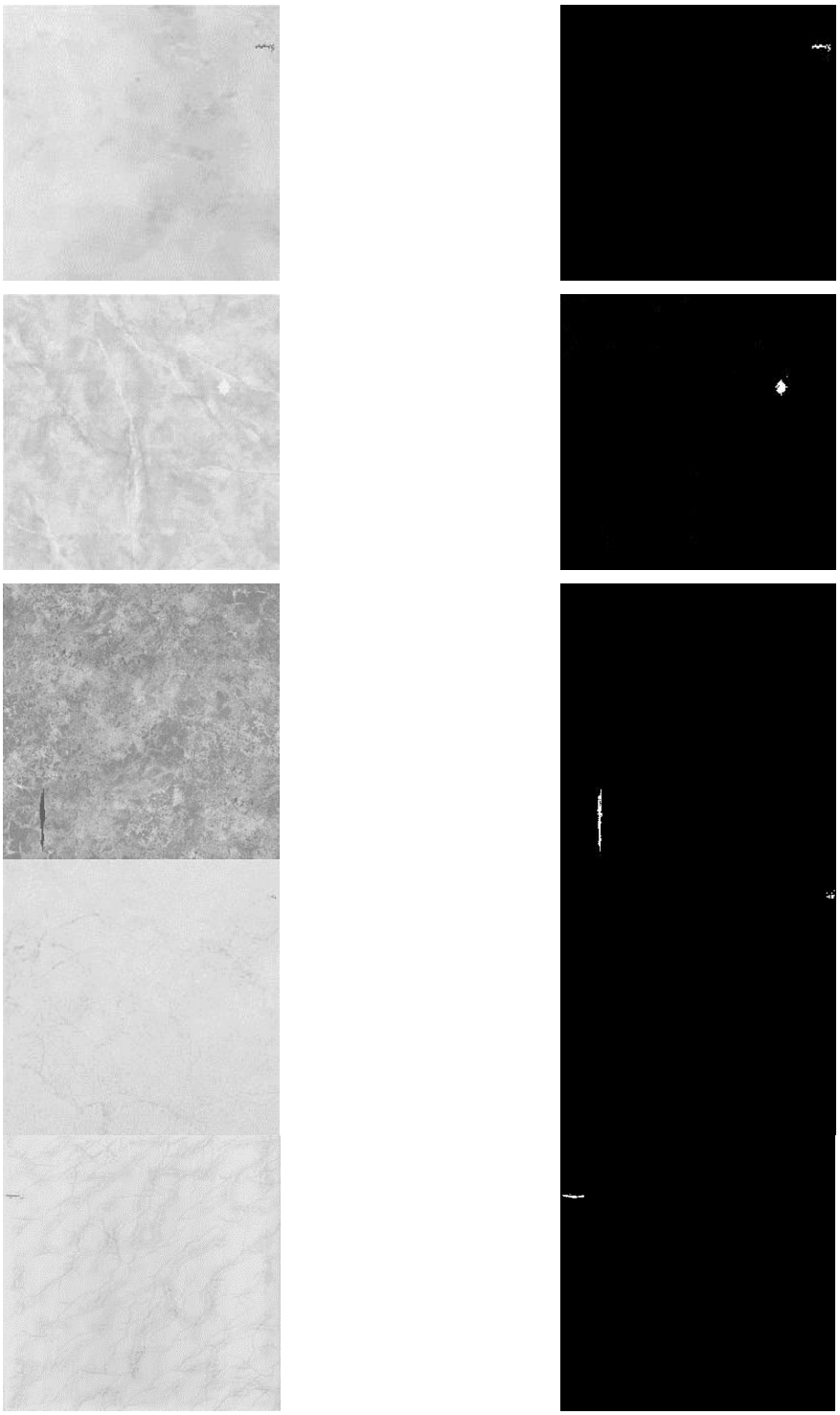

Figure 8. Several examples of the application of the proposed method on the random textures of defective tiles.

These three criteria are defined as the following equations:

$$Sensitivity = \frac{TP}{TP + FN} \times 100\% \quad (28)$$

$$Specificity = \frac{TN}{TN + FP} \times 100\% \quad (29)$$

$$Accuracy = \frac{TN + TP}{TN + FP + FN + TP} \times 100\% \quad (30)$$

In these equations,

TP indicates the *True Positives*, i.e., the number of defective pixels that have been detected correctly.

TN indicates the *True Negatives*, i.e., the number of flawless pixels that have been detected correctly.

FP indicates the *False Positives*, i.e., the number of flawless pixels that have been detected incorrectly as defective ones.

FN indicates the *False Negatives*, i.e., the number of defective pixels that have been detected incorrectly as flawless ones.

By applying the above three criteria on all the existing database images, the accuracy and the quality of the proposed method can be determined. Table 1 shows the effectiveness of the proposed approach by the three introduced criteria. Also, to compare the proposed method with the other approaches in terms of accuracy and efficiency, the methods of Gray-Level TEXEM [6] and Gray-Level T^2 [7] have been implemented, and the results of applying the above three measures have been given in Table 1.

As is observed in Table 1, the highest accuracy belongs to the TEXEM method [6], the highest specificity is achieved by the proposed method, and the highest sensitivity again belongs to the TEXEM approach [6].

Also from a computational perspective, the proposed method and the Gray-Level TEXEM [6] and Gray-Level T^2 [7] approaches have been applied on the set of database images, and the average processing times at the training and testing stages have been listed in Table 2. It should be mentioned that the proposed method has been executed in the MATLAB software environment, on a 2.8 GHz processor, with 6GB of ram.

Table 1. Performance of proposed method in comparison with [6] and [7].

Method	Sensitivity	Specificity	Accuracy
Proposed Method	91.3%	94.4%	92.85%
Gray-Level TEXEM	92.4%	93.9%	93.15%
Gray- Level T^2	90.1%	84.9%	87.5%

As Table 2 indicates, the processing time in the proposed method, both at the training and testing stages, is faster than that in the other two methods. This computational characteristic makes the proposed method more suitable for industrial implementations

rather than the other introduced methods. An important reason for a shorter computation time at the training stage in the proposed method, compared to the TEXEM method, is that the feature vectors of the flawless texture are less scattered in the proposed method; and the less scattered the model parameters are from each other, the quicker the convergence of the EM algorithm will be [20]. As pointed out in the previous section, determining the exact number of Gaussian mixtures has a significant impact on the processing time and the accuracy of the proposed algorithm. For the sake of comparison, the accuracy and the processing time of the proposed algorithm with respect to the number of Gaussian mixtures (k) have been listed in Table 3.

Table 2. The processing time in training and testing stages

Method	Training Stage	Testing Stage
Proposed Method	20 sec.	7 sec.
Gray-Level TEXEM	110 sec.	11 sec.
Gray- Level T^2	190 sec.	26 sec.

Table 3. The processing time and accuracy of proposed method based on number of different Gaussian mixtures.

Number of Gaussian mixture	Accuracy	Process time in testing stage	Process time in training stage
K = 3	71.3%	2 sec	7 sec
K = 4	75.7%	3sec	9sec
K = 5	83.2%	5 sec	13 sec
K = 6	86.1%	6 sec	16 sec
K = 8	92.85%	9 sec	26 sec
K = 9	92.86%	15 sec	31 sec
K = 10	92.86%	18 sec	37 sec

5. Conclusion

In this paper, a new method was presented for the automatic detection and localization of the defects of random textures in grayscale images with the help of the Gaussian mixture model and the optimal response of Gabor filter.

The proposed method was compared with the recent approaches presented for the detection of defects in random textures, both in terms of accuracy and computational volume. This comparison was carried out by applying all the three mentioned methods on a database of textural images from ceramic tile surfaces. In this databank, there were ten different textural families with various defects of different sizes. Since in many practical applications, such as the automatic visual surface inspection, the real-time implementation capability of a texture defect detection method is of high importance, therefore, the computational volume and cost of the noted method will have a major influence on its performance and effectiveness. Hence, the three mentioned methods were also compared from the standpoint of computational efficiency. It was observed that the processing time in the proposed method, both at the training and testing stages, is faster than the other methods; and this advantage, in addition to its efficient performance, makes the proposed method an appropriate candidate for industrial implementation. It should be mentioned that in this paper, the mentioned methods have been applied on the images of ceramic tile surfaces; however, these methods can also be applied on any other random texture such as the surfaces of wood, leather or even textiles and organic tissue textures. The proposed method has been basically designed for the detection of defects in grayscale surface textures, and the detection of defects in color textures constitutes a generalization of the grayscale case; because in this regard, the grayscale approach can be separately applied to every color channel.

References

[1] MT. Hayajneh, AM. Hassan, F. Al-Wedyan, "Monitoring defects of ceramic tiles using fuzzy subtractive clustering-based system identification method," *Soft Computing*, vol. 14, no. 6, pp. 615-626, 2010.

[2] Ngan HYT, Yung NHC, Pang GKH. "Performance Evaluation for Motif-Based Patterned Texture Defect Detection," *IEEE Transactions on Automation Science and Engineering*, 7: 58 – 72, 2010.

[3] Tsai DM, Luo JU, "Mean Shift-Based Defect Detection in Multicrystalline Solar Wafer Surfaces," *IEEE Transactions on Industrial Informatics*, 7: 125 – 135, 2011.

[4] Mirmehdi M, Xie X, Suri J. Handbook of Texture Analysis 2008.

[5] Lopez F, Prats J.M, Ferrer A, Valiente JM. Defect Detection in Random Color Textures using the MIA T2 Defect Maps. *Journal of Image Analysis and Recognition*, 752-763, 2006.

[6] X. Xie, M. Mirmehdi, "TEXEM: Texture exemplars for defect detection on random textured surfaces," *IEEE Transactions on Pattern Analysis and Machine Intelligence*, 29: 1454–1464, 2007.

[7] Hadizadeh H, Shokouhi SHB. Random Texture Defect Detection using 1-D Hidden Markov Models based on Local Binary Patterns. *Transactions on Information and Systems*, 7: 1937-1945, 2008.

[8] Aborisade DO, Ojo JA. Novel Defect Segmentation Technique in Random Textured Tiles. *International Journal of Scientific and Engineering Research* 2011.

[9] Riaz, F, Hassan, A, Rehman, S, Qamar, U. Texture Classification Using Rotation- and Scale-Invariant Gabor Texture Features. *IEEE Signal Processing Letters*, 20: 607 - 610, 2013.

[10] Alimohamadi H, Ahmadyfard A, Shojaee E. Defect Detection in Textiles Using Morphological Analysis of Optimal Gabor Wavelet Filter Response. *IEEE International Conference on Computer and Automation Engineering*; pp. 26 – 30, 2009.

[11] Montoya j, Leite NJ, Torres R. Wavelet-based fingerprint image retrieval. *Journal of Computational and Applied Mathematics*, vol. 227, pp. 294-307, 2009.

[12] Li Ma, Staunton R.C. Optimum Gabor filter design and local binary patterns for texture segmentation. *Pattern Recognition Letters* 2009; 29: 664-672.

[13] Abche AB, et.al. Image Registration of Radiographic Images Using an Elastic Approach. *IEEE Nuclear Science Symposium Conference Record*; pp. 2081 – 2085, 2006.
[14] W Li, Prasad S. Fowler J.E. "Hyperspectral Image Classification Using Gaussian Mixture Models and Markov Random Fields," *IEEE Geoscience and Remote Sensing Letter*, 11: 153-157, 2014.
[15] Varma M, Zisserman A. "Texture classification: Are filter banks necessary?," *In IEEE Conf. on Computer Vision and Pattern Recognition*, pp. 691–698, 2003.
[16] Xian GM. An identification method of malignant and benign liver tumors from ultrasonography based on GLCM texture features and fuzzy SVM," *Expert Systems with Applications*, 37: 6737-6741, 2010.
[17] D. Kim, P. Kang, S. Cho, H. Lee, S. Doh, "Machine learning-based novelty detection for faulty wafer detection in semiconductor manufacturing," *Expert Systems with Applications*, 39: 4075–4083, 2012.
[18] Monadjemi A, Mirmehdi M, Thomas BT. Restructured Eigenfilter Matching for Novelty Detection in Random Textures. *In Proceedings of the 15th British Machine Vision Conference*, pp. 637-646, 2004.
[19] L. Shen, S. Jia, Z. Ji, W. Chen, "Extracting local texture features for image-based coin recognition," *IET Image Processing*, vol. 5, pp. 394-401, 2011.
[20] F. Saâdaoui, "Acceleration of the EM algorithm via extrapolation methods: Review, comparison and new methods," *Computational Statistics & Data Analysis*, vol. 54, pp. 750–766, 2010.